Aerosol indirect effect on tropospheric ozone via lightning

Tianle Yuan,[1,2] Lorraine A. Remer,[1] Huisheng Bian,[1,3] Jerald R. Ziemke,[3,4] Rachel Albrecht,[5] Kenneth E. Pickering,[3] Lazaros Oreopoulos,[2] Steven J. Goodman,[6] Hongbin Yu,[2,7] and Dale J. Allen[8]

Received 1 March 2012; revised 8 August 2012; accepted 17 August 2012; published 26 September 2012.

[1] Tropospheric ozone (O_3) is a pollutant and major greenhouse gas and its radiative forcing is still uncertain. Inadequate understanding of processes related to O_3 production, in particular those natural ones such as lightning, contributes to this uncertainty. Here we demonstrate a new effect of aerosol particles on O_3 production by affecting lightning activity and lightning-generated NO_x (LNO_x). We find that lightning flash rate increases at a remarkable rate of 30 times or more per unit of aerosol optical depth. We provide observational evidence that indicates the observed increase in lightning activity is caused by the influx of aerosols from a volcano. Satellite data analyses show O_3 is increased as a result of aerosol-induced increase in lightning and LNO_x, which is supported by modle simulations with prescribed lightning change. O_3 production increase from this aerosol-lightning-ozone link is concentrated in the upper troposphere, where O_3 is most efficient as a greenhouse gas. In the face of anthropogenic aerosol increase our findings suggest that lightning activity, LNO_x and O_3, especially in the upper troposphere, have all increased substantially since preindustrial time due to the proposed aerosol-lightning-ozone link, which implies a stronger O_3 historical radiative forcing. Aerosol forcing therefore has a warming component via its effect on O_3 production and this component has mostly been ignored in previous studies of climate forcing related to O_3 and aerosols. Sensitivity simulations suggest that 4–8% increase of column tropospheric ozone, mainly in the tropics, is expected if aerosol-lighting-ozone link is parameterized, depending on the background emission scenario. We note, however, substantial uncertainties remain on the exact magnitude of aerosol effect on tropospheric O_3 via lightning. The challenges for obtaining a quantitative global estimate of this effect are also discussed. Our results have significant implications for understanding past and projecting future tropospheric O_3 forcing as well as wildfire changes and call for integrated investigations of the coupled aerosol-cloud-chemistry system.

Citation: Yuan, T., L. A. Remer, H. Bian, J. R. Ziemke, R. Albrecht, K. E. Pickering, L. Oreopoulos, S. J. Goodman, H. Yu, and D. J. Allen (2012), Aerosol indirect effect on tropospheric ozone via lightning, *J. Geophys. Res.*, *117*, D18213, doi:10.1029/2012JD017723.

1. Introduction

[2] Tropospheric ozone (O_3) plays a key role in atmospheric chemistry, air quality, and radiative balance as an oxidant [*Thompson*, 1992] and a greenhouse gas [*Solomon et al.*, 2007]. It is formed by photochemical oxidation of carbon monoxide (CO) and hydrocarbons in the presence of nitrogen oxides (NO_x) in the troposphere. Human activities have significantly increased these ozone precursors, which has resulted in a substantial increase in tropospheric ozone concentration [*Logan*, 1985; *Marenco et al.*, 1994; *Lelieveld et al.*, 2004; *Oltmans et al.*, 2006]. Anthropogenic O_3 increase and the corresponding radiative forcing are calculated using Chemical Transport Models (CTMs) by

[1]Joint Center for Environmental Technology, University of Maryland, Baltimore County, Baltimore, Maryland, USA.
[2]Climate and Radiation Laboratory, NASA Goddard Space Flight Center, Greenbelt, Maryland, USA.
[3]Atmospheric Chemistry and Dynamics Laboratory, NASA Goddard Space Flight Center, Greenbelt, Maryland, USA.
[4]Goddard Earth and Sciences Technology and Research, Morgan State University, Baltimore, Maryland, USA.
[5]Instituto Nacional de Pesquisas Espaciais, DSA/CPTEC, Cachoeira Paulista, Brazil.
[6]NOAA/NESDIS, NASA Goddard Space Flight Center, Greenbelt, Maryland, USA.
[7]Earth System Science Interdisciplinary Center, University of Maryland, College Park, Maryland, USA.
[8]Department of Atmospheric and Oceanic Science, University of Maryland, College Park, Maryland, USA.

Corresponding author: T. Yuan, NASA/Goddard Space Flight Center, Bldg. 33, Room A306, Greenbelt, MD 20771, USA. (tianle.yuan@nasa.gov)

0148-0227/12/2012JD017723

differentiating current and background O_3 levels. By removing known anthropogenic emissions, natural background O_3 can be inferred and the radiative forcing by anthropogenic O_3 can then be calculated. State-of-the-art CTMs can simulate current global O_3 distributions while the simulated background O_3 is constantly higher than surface measurements made over a century ago [*Bojkov*, 1986; *Volz and Kley*, 1988; *Marenco et al.*, 1994; *Wang and Jacob*, 1998]. Determining the natural background O_3 concentration becomes a key source of uncertainties along with other factors for assessing O_3 forcing [*Wang and Jacob*, 1998; *Hauglustaine and Brasseur*, 2001; *Lamarque et al.*, 2005; *Gauss et al.*, 2006; *Horowitz*, 2006; *Stevenson et al.*, 2006; *Wild*, 2007].

[3] Natural sources of O_3 precursors include NO_x from soil and lightning, CO from natural fire and methane oxidation, and hydrocarbons from vegetation and ocean. Lightning-generated NO_x (LNO_x), typically released in the middle to upper troposphere [*Pickering et al.*, 1998; *Ott et al.*, 2010], is crucial for the formation of the upper tropospheric O_3. O_3 in this layer of atmosphere is particularly efficient as a greenhouse gas. Upper tropospheric O_3 formation is also particularly sensitive to LNO_x because of a combination of the low background concentration and long lifetime of NO_x in the upper troposphere [*Lamarque et al.*, 1996; *Hauglustaine et al.*, 2001; *Tie et al.*, 2001; *Martin et al.*, 2007; *Ott et al.*, 2010], especially in the tropics where anthropogenic sources are sparse [*Schumann and Huntrieser*, 2007; *Labrador et al.*, 2005; *Sauvage et al.*, 2007; *Lamarque et al.*, 2010]. As such, LNO_x is instrumental in understanding the dominant features in tropical tropospheric O_3 distribution [*Thompson et al.*, 2000; *Edwards et al.*, 2003; *Thompson et al.*, 2003; *Sauvage et al.*, 2007; *Martin et al.*, 2002b]. Even over and downwind of midlatitude continents where anthropogenic sources are strongest LNO_x is critical in summertime O_3 formations in the upper troposphere [*Zhang et al.*, 2003; *Cooper et al.*, 2006; *Allen et al.*, 2010]. Much less well known, however, is the accurate source strength of LNO_x and its variability since the preindustrial time [*Mickley et al.*, 2001; *Schumann and Huntrieser*, 2007]. The source strength of LNO_x, regardless of its uncertainty, has been mostly assumed constant with time because lightning is considered a natural process with no clear mechanisms that link its frequency to human activity at large scales [*Schumann and Huntrieser*, 2007].

[4] It has been proposed that aerosols can change lightning activity [*Lyons et al.*, 1998; *Mickley et al.*, 2001; *Altaratz et al.*, 2010; *Yuan et al.*, 2011; *Sherwood et al.*, 2006]. This possibility has been under debate for some time [*Williams et al.*, 2002; *Williams*, 2005]. However, a causal aerosol-lightning link is difficult to prove due to the strong coupling between meteorology, deep convection, lightning and aerosol concentration [*Williams et al.*, 2002]. For example, if meteorology is responsible for both the aerosol and lightning anomaly the correlation between aerosol and lightning could not be attributed to a physical cause. Recently, we provide strong evidence of aerosols enhancing lightning activity of tropical oceanic clouds, which avoids the convolution [*Yuan et al.*, 2011] (also see more discussions in the following). Physically, more aerosols are shown to delay/suppress the warm rain by increasing number of cloud droplets and decreasing droplet size, enhance cloud mixed-phase activity, invigorate convection and increase lightning frequency of pristine maritime cumulonimbus clouds [*Yuan et al.*, 2011]. Similar effects seem to exist for anthropogenic biomass burning aerosols over land [*Lyons et al.*, 1998; *Altaratz et al.*, 2010; *Albrecht et al.*, 2011]. In light of the physical link between aerosol and lightning, lightning activity and LNO_x can no longer be assumed to be constant in the face of anthropogenic aerosol changes.

[5] Here we explore and assess potential links among aerosol loading, lightning frequency and concentrations of O_3 and its precursors using a suite of satellite data together with a CTM, the Global Modeling Initiative (GMI) [*Duncan et al.*, 2007; *Allen et al.*, 2010]. We first focus our analysis on a specific region east of the Philippines (from 125°E to 150°E and from 5°N to 20°N) where increased lightning is related to enhanced aerosol loading from the Anatahan volcano (16.35°N, 145.7°E) [*Yuan et al.*, 2011]. Global implications are assessed with conceptual model sensitivity experiments. In section 2, we introduce the data sets and the model used in this study. In section 3, we present results regarding the validity of associations among aerosol, lightning and O_3 with satellite data analysis as well as numerical model simulations. Sensitivity model experiment results are also provided in this section. In section 4, we discuss the potential uncertainties, challenges and implications for future studies. Summary is provided in section 5.

2. Data and Model

2.1. Data Sets

[6] In this study we utilize a suite of satellite data sets that characterize aerosol, gas and lightning. For aerosols we use aerosol optical depth (AOD) from the Moderate resolution Imaging and Spectroradiometer (MODIS) product [*Remer et al.*, 2005) (from 2000 to 2009) and Global Aerosol Climatology Project (GACP) [*Geogdzhayev et al.*, 2005] as a proxy for aerosol loading. Collection 005 MODISlevel 2 (daily) and level 3 (monthly) aerosol products are both used. Level 3 monthly products are in $1^\circ \times 1^\circ$ resolution and the native resolution for Level 2 product is 10 km. We used aerosol optical depth at 550 nm and aerosol Angstrom exponent in the visible. The GACP product we used is monthly mean data at $1^\circ \times 1^\circ$ spatial resolution. The data set is available from 1982 to 2005.

[7] The flash rate density is computed from the Tropical Rainfall Measurement Mission (TRMM) Lightning Imaging Sensor (LIS) total lightning global data set corresponding to the MODIS 2000–2009 time period. The LIS was launched in 1997 into a low inclination earth orbit of 35° at an altitude of 350 km, later raised to 402 km in August 2001 to extend the mission lifetime. From this altitude the LIS observed total (in-cloud and cloud-to-ground) lightning from the individual storms within in its 600 km × 600 km field-of-view for about 90 s. The LIS orbit data were binned into $0.25^\circ \times 0.25^\circ$ grids accounting for the total view time the sensor observed the Earth and the total number of flashes detected. LIS flashes were then corrected by the instrument detection efficiency [*Boccippio et al.*, 2002]. Monthly flash rate densities (fl km^{-2} $month^{-1}$) were calculated by a cumulative method (sum of all flashes in a month in a grid cell divided by the sum of LIS view time in the same grid

cell). Finally, seasonal flash rate density was computed by averaging the monthly flash rate densities.

[8] For gases, NO_2 measurements from the Ozone Monitoring Instrument (OMI) [*Bucsela et al.*, 2006] (2004–2009) are our main data source. They are taken as a NO_x proxy. Additional NO_2 data sets from three groups are used for consistency check. The Dutch Tropospheric Emission Monitoring Internet Service (TEMIS) team provide NO_2 retrievals from OMI, the Global Ozone Monitoring Experiment (GOME, 1996–2002) and SCanning Imaging Absorption SpectroMeter for Atmospheric CartograpHY (SCIAMACHY, 2002–2009) [*Boersma et al.*, 2004] with different algorithms [*Boersma et al.*, 2007; *Boersma et al.*, 2008]. A second SCIAMACHY NO_2 product is provided by Dr. Randall Martin's group at Dalhousie University [*Martin et al.*, 2002a, 2006]. A third NO_2 data source is column retrievals from GOME and SCIAMACHY produced by the University of Bremen group [*Richter and Burrows*, 2002]. The University of Bremen product derives an NO_2 anomaly instead of direct column concentration. Different data sets are examined here to check the robustness of our results. Because these data are derived from different sensor and/or different retrieval algorithms consistency using different NO_2 products increases our confidence in our results.

[9] For O_3 we use tropospheric O_3 concentration retrieved from TOMS [*Ziemke et al.*, 1998] (1979 to 2005 with a brief break between 1994 and 1996) and from the combination of OMI and Microwave Limb Sounder (MLS) [*Ziemke et al.*, 2006] (2004–2009). We use monthly data at $5^\circ \times 5^\circ$ and $1^\circ \times 1.25^\circ$ (latitude by longitude) resolution for TOMS and OMI/MLS, respectively. Due to methodological constraints, TOMS data cover only the tropical belt from 15°S to 15°N while OMI/MLS data cover the latitudinal band between 60°S and 60°N. An advantage of TOMS O_3 is that measurements are less prone to instrument absolute calibration errors because it is a differential method using a single instrument to derive tropospheric ozone (i.e., tropospheric ozone = TOMS total ozone minus TOMS stratospheric ozone, this single-instrument differencing removes any potential instrument measurement bias or drift for TOMS). Instrument calibration problems are also alleviated for OMI/MLS since stratospheric ozone from OMI is used to cross-adjust MLS stratospheric ozone prior to deriving the tropospheric ozone residual product (i.e., tropospheric ozone = OMI total ozone minus MLS adjusted stratospheric ozone).

[10] Other trace gases such as SO_2 from OMI and CO from Measurements of Pollution in the Troposphere (MOPITT) and Atmospheric Infrared Sounder (AIRS) are used to characterize air mass.

2.2. Model

[11] The NASA Global Modeling Initiative (GMI) chemical transport model includes a combined stratosphere-troposphere chemical mechanism with 124 species, 322 chemical reactions, and 81 photolysis processes [*Duncan et al.*, 2007]. The tropospheric portion of the chemical mechanism includes a detailed description of tropospheric ozone, NO_x, and hydrocarbon photochemistry. It has been updated with recent experimental data and data for the quenching reactions of $O(^1D)$ by N_2, O_2, and H_2O. It is integrated using the SMVGEAR II algorithm [*Jacobson*, 1995]. Photolysis rates in the troposphere and stratosphere are calculated using the Fast-JX radiative transfer algorithm [*Wild et al.*, 2000; *Bian and Prather*, 2002], an efficient algorithm that calculates photolysis rates in the presence of an arbitrary mix of cloud and aerosol layers. The scheme treats both Rayleigh scattering as well as Mie scattering by clouds and aerosol. Heterogeneous chemistry and effects of aerosols on photochemistry are considered [*Jacobson*, 1995]. Lightning flash rate in GMI is based on upward convective flux in the upper troposphere (around 400 mb) [*Allen et al.*, 2010]. The magnitude of lightning rate is constrained by observation on a grid scale and this approach gives good fit to the climatology of observed lightning distribution.

[12] CMIP5 historical 1850 emissions of anthropogenic, biomass burning, and ship for both gas and aerosol tracers are used [*Lamarque et al.*, 2010]. There was no aircraft emission at that year. The continuously erupting volcanic SO2 emission and oceanic DMS emission are also included. The emissions of 2005 used in this work are constructed from various emission inventories. The anthropogenic and shipping emissions of CO, NOx, and non-methane hydrocarbons (NMHC) are described in *Duncan et al.* [2008] and their biofuel and biomass burning emissions are given in *Duncan et al.* [2007]. The biogenic emissions simulated in GMI use MEGAN algorithm [*Guenther et al.*, 1995, 2006]. The emissions of aerosols and their precursors follow the work of *Bian et al.* [2009] and *Chin et al.* [2009]. The model accounts for time-varying emissions from anthropogenic, biomass burning, biogenic, and volcanic sources for possible BC, OC, SO2, NH3 and calculates wind-blown dust and sea salt emissions using the GEOS-4 meteorological fields. The GEOS-4 drives the GMI tracer transport as well. The volcanic SO_2 emission from the volcano in our study has not been included in the emission data set yet. A future study may include interactive aerosols including updated SO2 emissions from volcanoes.

[13] GMI will be used in this study to carry out sensitivity studies on how lightning changes affect tropospheric ozone chemistry. Specifically, we will examine how a fivefold increase of lightning over our study region [5°N∼20°N, 125°E∼150°E] might affect tropospheric ozone production. The increase is meant to mimic what is observed from satellite. In addition, we will use the GMI model to speculate on the global impact of aerosol induced lightning change for tropospheric ozone historical variation and climate forcing. We will determine the lightning difference between 1850 and 2005 based on extrapolation of observed aerosol-lightning frequency relationships. We then impose the aerosol-induced lightning difference on atmospheres with 1850 and 2005 emission scenarios to gauge the possible range of impact on O_3.

3. Results

[14] Despite the frequent occurrence of deep convective clouds, lightning activity is usually quite low in our study region, which is true for other oceanic areas with weakly electrified storms having weaker vertical motions and less well-developed mixed-phase precipitation regions aloft than their continental counterparts [*Christian et al.*, 2003, *Zipser et al.*, 2006; *Goodman et al.*, 2007]. We call this a 'scarce lightning ample convection (SLAC)' conundrum. As a result, O_3 concentration during June–July–August (JJA) for the

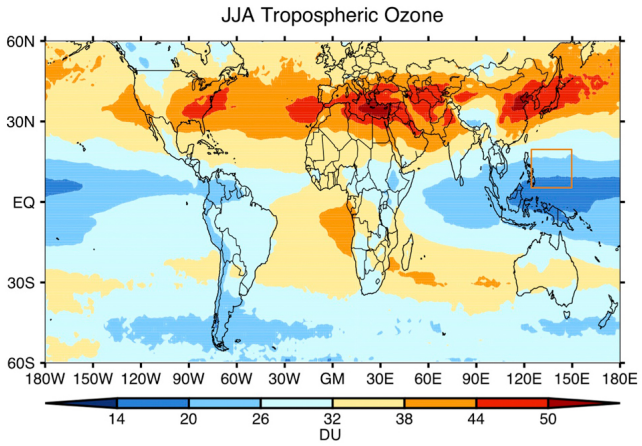

Figure 1. OMI tropospheric ozone JJA 'climatology' (mean of 2004–2009) [*Ziemke et al.*, 2006]. Peak values are observed over and downwind of northern midlatitude population centers. In the tropics Western Pacific is the minimum while the South Atlantic has maximum value. The focus area of this study is outlined with a rectangular box.

region of interest is typically very low (Figure 1) due to lack of lightning and anthropogenic NO_x sources as well as convective transport of O_3-depleted maritime boundary layer air [*Solomon et al.*, 2005]. But in 2005 the *areal mean* lightning activity is increased by 150%, which was linked to a 60% increase in aerosol loading resulting from a low-altitude volcanic source [*Yuan et al.*, 2011].

3.1. Characteristics of Changes in Aerosol and Lightning

[15] Here we provide further analysis on the corresponding distribution of changes in both aerosol and lightning. Figure 2a shows the spatial distribution of seasonal mean MODIS aerosol optical depth anomaly for JJA 2005. The climatology is based on JJA data between 2000 and 2009. The positive anomaly shapes like a plume originating from a point source situated at around 16°N and 145°E, the location of the Anatahan volcano that was actively spewing SO_2 gases during JJA of 2005 [*Yuan et al.*, 2011]. The anomaly ranges from 0.05 to greater than 0.2 units representing an increase of 50–200% above the climatology. Figures 2b and 2c provide a qualitative view of the strong lightning increase associated with the aerosol anomalies. The lightning activity within the

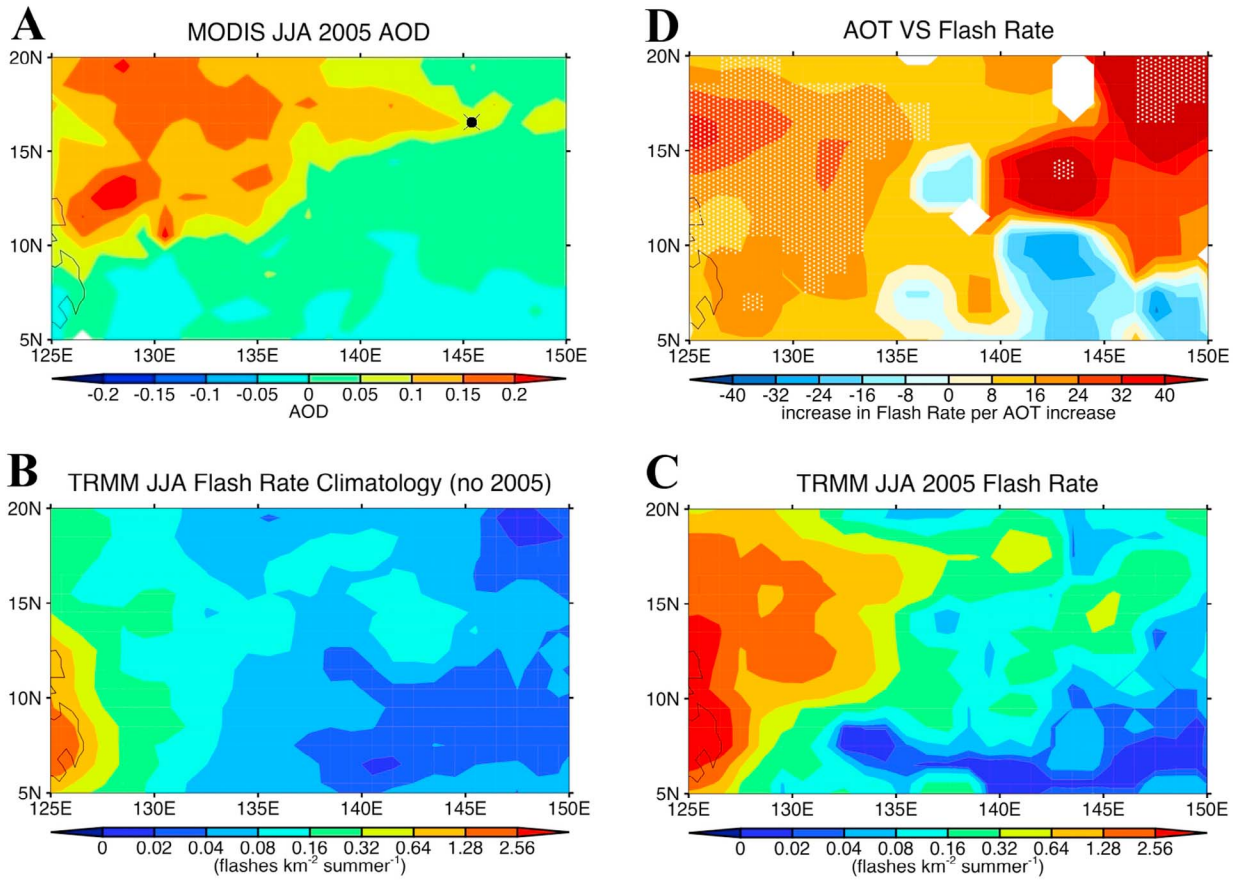

Figure 2. (a) Aerosol optical depth (AOD) anomaly map of June, July, and August of 2005 relative to climatology (2000–2009). We can see a plume like feature originating from the volcano at around 16°N and 145°E, marked by a star-dot. (b) The climatology of flash rate without 2005. Note the color scale is exponential. (c) The flash rate in 2005 with the same color bar as Figure 2b. (d) Increase in flash rate per unit of aerosol optical depth increase. The dotted areas represent where the correlation coefficient between flash rate and aerosol optical depth exceeds 95% confidence level. We applied 2 × 2 window smoothing in Figures 2b, 2c, and 2d.

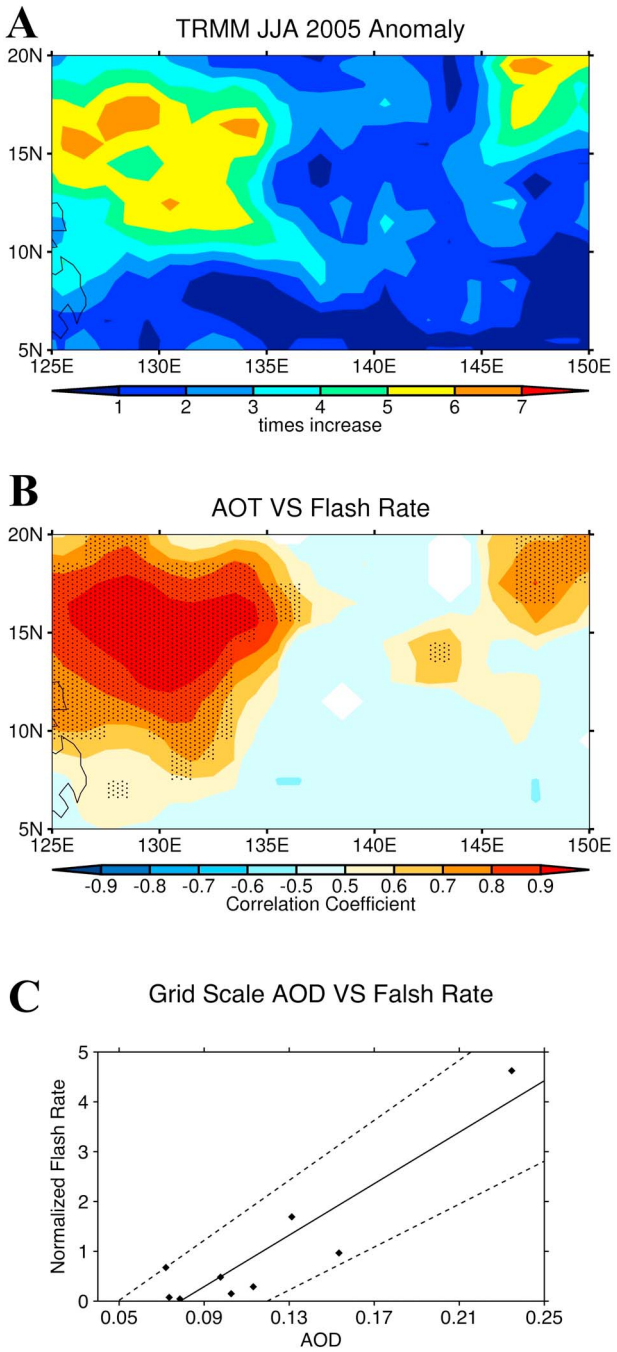

Figure 3. (a) The ratio between flash rates of JJA 2005 and that of the climatology between 1998 and 2007. The majority of increase is between 5 and 7 times over areas where the correlation between AOD and flash rate is statistically significant at 95% level (Figures 2d and 3b). (b) Map of correlation coefficients between times series of AOD and flash rate at every grid point. The stippled (black dots) areas are statistically significant at 95% level. Three by 3 window smoothing is applied in both cases. (c) A scatterplot between AOD and normalized flash rate (by the climatological average on the grid point of 130 E and 11 N). The dashed lines represent one-sigma uncertainty of the fitted line. All points are within these two lines.

aerosol plume in JJA of 2005 (Figure 2c) is much higher than the climatological mean level (Figure 2b), noting the color scales. Flash rate density over heavily aerosol affected maritime areas is almost on par with that of the Philippine Islands more than 500 km to the west (Figure 2c). The seasonal mean lightning flash rate density increases as much as 700% or more in areas of 150% aerosol anomalies. The spatial distribution of lightning increase also follows well that of the aerosol anomaly (Figure 3a). We quantify the aerosol-lightning relationship by calculating the correlation between seasonal mean of aerosol optical depth and lightning flash rate density in each 1° box. An example for the grid of 130E and 11 N is given in Figure 3c, which is a typical grid with a moderate correlation coefficient value. Statistically significant ($p < 0.05$) correlations are found over many boxes and on average the flash rate density increases at a rate of 20–40 times per unit increase of aerosol optical depth (Figures 2d and 3b). These results are important since typical flash densities over maritime areas are almost an order of magnitude smaller than that of maritime continents (Figure 2b) [*Zipser et al.*, 2006; *Goodman et al.*, 2007] while flash rates over polluted maritime locations in 2005 are comparable to those over the Philippines Islands. The land-ocean contrast in aerosol optical depth is about 0.2 between the Philippines Islands and the oceanic areas [*Remer et al.*, 2005], which would translate into a 6 to eightfold increase in lightning activity if we use the lightning-AOD ratios derived from Figure 2d. Results here suggest, at least over this area, aerosols are responsible for a large part of the land-ocean contrast in lightning activity.

3.2. Examination of Alternative Hypotheses

[16] How do we know that aerosol increase in 2005 is causing the enhanced lightning activity, which can be also affected by meteorological factors and inter-annual variability caused by El Nino and La Nina [*Yuan et al.*, 2011; *Goodman et al.*, 2000; *Williams and Stanfill*, 2002; *Chronis et al.*, 2008]? To add further evidence that meteorological factors were not responsible for the changes beyond what is presented in [*Yuan et al.*, 2011], we first apply a lightning parameterization based on assimilated meteorology [*Allen and Pickering*, 2002]. The parameterization is based on upward convective mass flux calculated from global reanalysis fields at every 3 h [*Allen et al.*, 2010]. If meteorological factors are responsible for the observed enhanced lightning anomaly and the reanalysis data can reasonably capture this variability, this approach would reflect these meteorology related changes. We find no strong increase in computed flash rate density using the convective flux approach in JJA 2005 compared to other years.

[17] Second, we carry out an observation-based analysis of what nature was doing in 2005. Within our domain we compute the number of potentially 'lightning-producing convective storms' in each JJA season using TRMM radar data. Two definitions are used for these storms in our study. In one definition, we use the official product information on whether a radar echo belongs to a convective or stratiform precipitation/cloud system and we only include those convective echoes that extend to higher than 5 km in height. The number of such convective events is then calculated by examining all oceanic observations in our region of interest. In the other definition, we include all radar pixels (i.e., both

Table 1. The Time Series of Number of Convective Events by Definition 1

	TRMM								
	1999	2000	2001	2002	2003	2004	**2005**	2006	2007
Number of events	1,169,720	1,111,366	966,511	978,411	955,464	1,034,762	**1,074,536**	1,031,071	901,152

convective and stratiform echoes) whose heights are equal to or greater than 5 km and have a reflectivity of at least 20dbz. The number of events is then again calculated for our region of interest. By carrying out this exercise we want to check whether the increased lightning activity in 2005 is simply due to more active and thus higher number of deep convection events. Both definitions gave a close to average (less than 5% higher than mean and within one standard deviation of mean) number of convective storms in JJA 2005 and the numbers for definition one are shown in Table 1. We note that the slightly higher value in 2005 could be partially due to the aerosol invigoration effect as discussed in *Yuan et al.* [2011]. Results do not change if we increase or decrease the threshold of altitude. This observationally based analysis suggests that in nature the number of potentially lightning-producing convective events did not significantly exceed the average in 2005. This again suggests that meteorological factors are not the dominant control on the anomalous number of flashes observed in 2005. Rather, it is the change in internal structure of convective storms that likely made them more active in lightning generation [*Yuan et al.*, 2011].

[18] Finally, we composite daily observations in JJA 2005 based on aerosol loading to investigate intraseasonal variations. In this analysis we use daily areal mean MODIS aerosol optical depth data and separate the days in JJA 2005 into two categories: high aerosol or low aerosol. We use fixed values of 0.25 and 0.15 as thresholds for high aerosol and low aerosol days, respectively, to get approximately equal sample sizes. This exercise serves as a random test at the intraseasonal scale since the volcanic aerosol source has no systematic dependence on dynamical and thermodynamical conditions. If we consider the areal mean of the whole region we find higher mean lightning count in high aerosol days than that of low aerosol days (the difference is statistically significantly at 99% confidence level). This is true no matter if we use Terra or Aqua data. For example, the mean flash count is 41 for high aerosol days as compared to 33 for low aerosol days if we use Terra MODIS. The numbers become 33 and 24, respectively, if Aqua MODIS is used (note that the sample days are changed when using these two data sets because of aerosol sampling differences). Since we know that most convection and lightning happen over the area west of 135°E (Figure 2) we repeated the exercise for the area bounded by 5°N and 20°N and 125°E and 135°E. The numbers are 26 and 13 for Terra MODIS and they are 27 and 19 for Aqua MODIS. In any case, high aerosol days have significantly higher lightning counts than those of low aerosol days.

[19] The year 2005 is not significantly different than the 10-year record in terms of the number of storms, nor in the meteorological environment in which those storms develop. The only exceptional factor in 2005 is the aerosols from volcanic activity that is independent of meteorology. Therefore, the physical mechanism that links aerosol, cloud properties and lighting activity provides the strongest explanation for the enhanced lightning in 2005. As shown in *Yuan et al.* [2011] aerosols decrease cloud droplet size, suppress warm precipitation and delay cloud glaciation [*Yuan and Li*, 2010; *Yuan et al.*, 2010], which invigorates convection, triggers more active mixed-phase process and leads to lightning increase.

3.3. Response in Chemistry

[20] Next we illustrate the ozone chemistry responses to the aerosol generated lightning anomaly. Lightning can generate NO_2 indirectly by releasing NO that is quickly oxidized into NO_2, which can be observed using satellite and/or in situ measurements [*Morris et al.*, 2010; *Beirle et al.*, 2010; *Bucsela et al.*, 2010]. Figure 4a shows the distribution of OMI-derived tropospheric NO_2 column amount anomaly based on JJA climatology of 2005–2009. The positive anomaly ranges from 0.3 to 0.9×10^{14} molecules/cm^2, which is 6–15% above the climatology depending on the location. Strong positive anomalies in NO_2 column amount in JJA 2005 are inside the area of positive aerosol and lightning anomalies. The areas of positive NO_2 anomaly occur over those of positive aerosol optical depth and lightning flash rate density anomalies [Figures 2 and 3]. Since satellite NO_2 retrievals cannot operate in a cloudy environment we note the observed changes are biased to clear sky values. This is why in model simulations we sample the data on the satellite orbit. We examine the robustness of the observed increase in NO_2 using data sets from other sensors (SCHIAMACHY, GOME, OMI) and/or algorithms (see section 2). We calculate the areal mean of tropospheric column NO_2 amount (or anomaly in the case of University of Bremen product) for each season. Results are shown in Table 2 where data sets from independent sensors and/or algorithms consistently indicate NO_2 concentration in JJA 2005 is the highest in the record. This is true even if data from GOME (data span from 1996 to 2003) are included (not shown here). There are some differences among results from different groups due to a host of factors that are beyond our scope of discussion here [*Boersma et al.*, 2004; *Martin et al.*, 2002a; *Richter and Burrows*, 2002], but they all confirm 2005 has the highest value. This consistency among different data sets increases our confidence in the robustness of results from OMI alone.

[21] We propose that the observed NO_2 increase results from increased lightning activity in JJA 2005. It will be demonstrated later that observed lightning increase can explain the observed NO_2 increase with a numerical model experiment, but could the observed NO_2 increase in 2005 arise from enhanced non-lightning sources, such as industrial and biomass burning emissions? If this were the case, we would expect elevated concentrations of combustion tracers such as CO. We use both MOPITT and AIRS CO data since they are sensitive to different vertical layers of the atmosphere. Both MOPITT and AIRS CO data show a

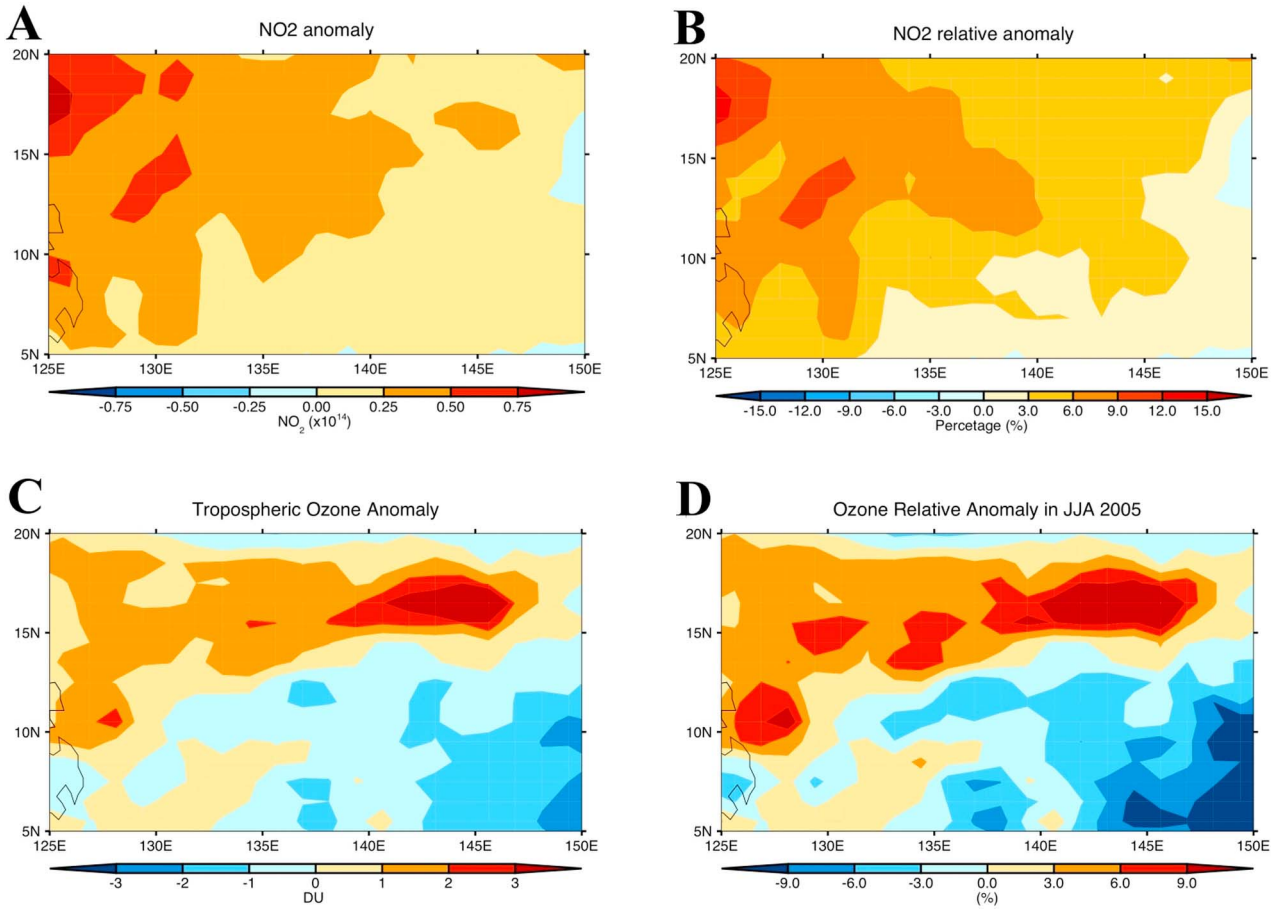

Figure 4. Anomaly maps of (a) tropospheric NO_2 and (c) tropospheric O_3 and (b and d) corresponding relative anomaly maps from OMI retrievals. Three by 3 smoothing is applied to Figures 4a and 4b.

slightly below average CO concentration in JJA 2005 over our area. Furthermore, we directly examine the strength level of upwind sources of pollution and/or biomass burning over places such as China and Indonesia. Figure 5 shows a larger scale view of the AOD anomaly (climatology is between 2000 and 2009) during JJA 2005. Major smoke source regions over Indonesia and Borneo have a negative aerosol optical depth anomaly during JJA of 2005, in contrast to the positive anomaly in our study region. The major pollution source over Eastern China is also below average. The dominant aerosol anomaly is the volcanically induced positive anomaly over usually pristine Western Pacific Ocean, which is almost all surrounded by negative anomalies. Similar results are also obtained using CO concentrations (not shown here). This analysis suggests that the AOD anomaly in our study region results from volcano activity, not from biomass burning smoke or industrial pollution. Thus we argue that lightning is the only observed parameter that could cause the increased NO_2.

[22] Figure 4c shows the tropospheric O_3 anomaly pattern in JJA 2005. The positive anomaly ranges from 1 to 2 Dobson Unit (DU, 1 DU = 2.69×10^{16} molecules cm^{-2}), about 3–6%, with a maximum exceeding 3 DU at the volcano, or about 10%. Since most LNO_x is produced in the middle to upper troposphere the increase in tropospheric O_3 should also be concentrated in the upper troposphere. The positive O_3 anomaly pattern just east of the Philippines (Figure 4d) (from 125°E to 135°E), where lightning is most active, occurs where anomalies of aerosol optical depth, lightning flash rate density and NO_2 column amount are also seen (Figures 2, 3, and 4). While some of the high O_3 anomaly at the volcano location might result from effect of volcanic ash on retrievals,

Table 2. Tropospheric NO_2 Retrievals Over Out Study Region From Three Different Groups[a]

	2003	2004	**2005**	2006	2007	2008	2009
NO_2 anomaly (University of Bremen)	−0.31	−0.24	**0.03**	−0.17	−0.50	−0.62	N/A
NO_2 ($\times 10^{14}$) (TEMIS)	−4.33	N/A	**10.39**	8.78	1.26	1.86	4.66
NO_2 ($\times 10^{14}$) (Randall Martin)	1.65	2.21	**3.35**	2.71	2.35	2.02	2.39

[a]We highlight the 2005 values in bold since they stand out as the highest values for all three time series. We note the negative values in Tables 2 mean that satellite observed whole column (including both tropospheric and stratospheric) NO_2 concentration is lower than transport model calculated stratospheric concentration [*Boersma et al.*, 2004]. The 2004 mean is not available because no quality measurements were made for June 2004 from one retrieval group.

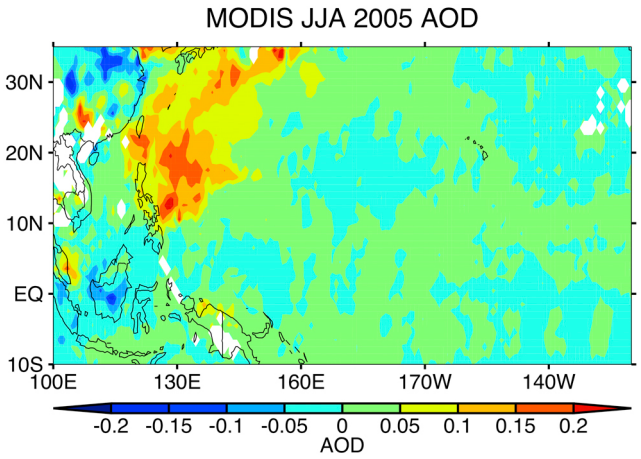

Figure 5. A large-scale view of AOD anomaly in JJA 2005. The volcano influence stands out in the map and its influence is not limited in our study region. AOD over major sources over China, Indonesia, Borneo etc., is below average in 2005.

volcanic ash is very unlikely to impact the retrievals west of 140°E. This is based on our analysis of OMI aerosol index data. Aerosol index provides a semiquantitative measure for both the presence and the loading of absorbing aerosols. The absorbing aerosols are important since they might affect O_3 retrieval if they are not properly accounted for, which will introduce uncertainty to the interpretation of observed O_3 patterns. Daily level-2 aerosol index data do not indicate high values in the region except for a weak maximum immediately downwind of the volcano. These maximum values only reach 1.5. Values around 1 or less are considered at or below the noise threshold level. No high values are found over the area west of 140°E. Therefore the absorbing ash close to the source region only weakly affects the O_3 retrievals at the same location and does not affect the overall result.

[23] Thus far the satellite observations are consistent with an aerosol-lightning-chemistry link, where aerosol affects convective cloud microphysics, alters lightning activity and LNO_x production, and subsequently affects tropospheric O_3 formation as a result. Next, we carry out numerical experiments to further explore the proposed link.

3.4. Modeling the Impact Over the Focus Region

[24] We investigate the proposed link using numerical simulations by the Global Modeling Initiative (GMI) chemical transport model. We will first focus on the limited study area and then conduct sensitivity test at a global scale. GMI does not explicitly resolve cloud and lightning processes, but does contain a full package of chemical reactions and a lightning NO_x parameterization scheme [*Allen et al.*, 2010]. Because of the missing cloud and lightning processes we cannot directly test the aerosol-lightning link. Instead, we mimic the observed lightning change (Figures 3a and 2c) by increasing oceanic lightning flash rate density in our study region by 5 times (5×). Figure 6b shows the NO_2 anomaly distribution as a result of the 5× increase in lightning. The magnitude and the spatial pattern of increase match the observation (Figure 4a). The spatial distribution of modeled increase of tropospheric O_3 (Figure 6a) also agrees reasonably well with that from observations (Figure 4d) although the magnitude is somewhat smaller. We note that the model run is only a sensitivity simulation to test the response of ozone and its precursors to lightning increase. The quantitative difference between modeled and observed O_3 is expected because of factors such as the sampling difference, and uncertainties in model physics (e.g., cloud and radiation processes), dynamics (e.g., stratosphere-troposphere exchange) and chemistry as well as in observation itself. For example, if we use a previous version of the OMI tropospheric O_3 product the observed O_3 increase is more than doubled, suggesting a more sensitive response. Model parameterization of convective transport process would have significant impact on the sensitivity of O_3 to lightning over this region [*Martin et al.*, 2002b]. Modeled cloud properties and its associated radiative effect on photolysis rates can also be an important source of uncertainties in simulations [*Tie et al.*, 2003; *Voulgarakis et al.*, 2009]. As such,

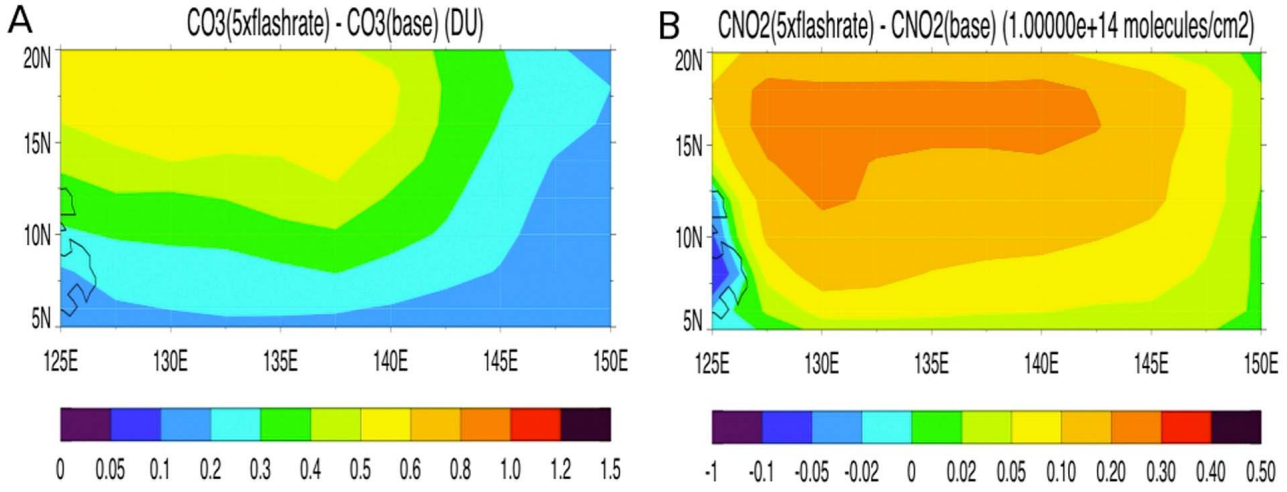

Figure 6. Modeled tropospheric (a) O_3 and (b) NO_2 changes when lightning flash rate of maritime convection is increased 5 times in our domain. The model data are sampled along the Aura satellite orbit.

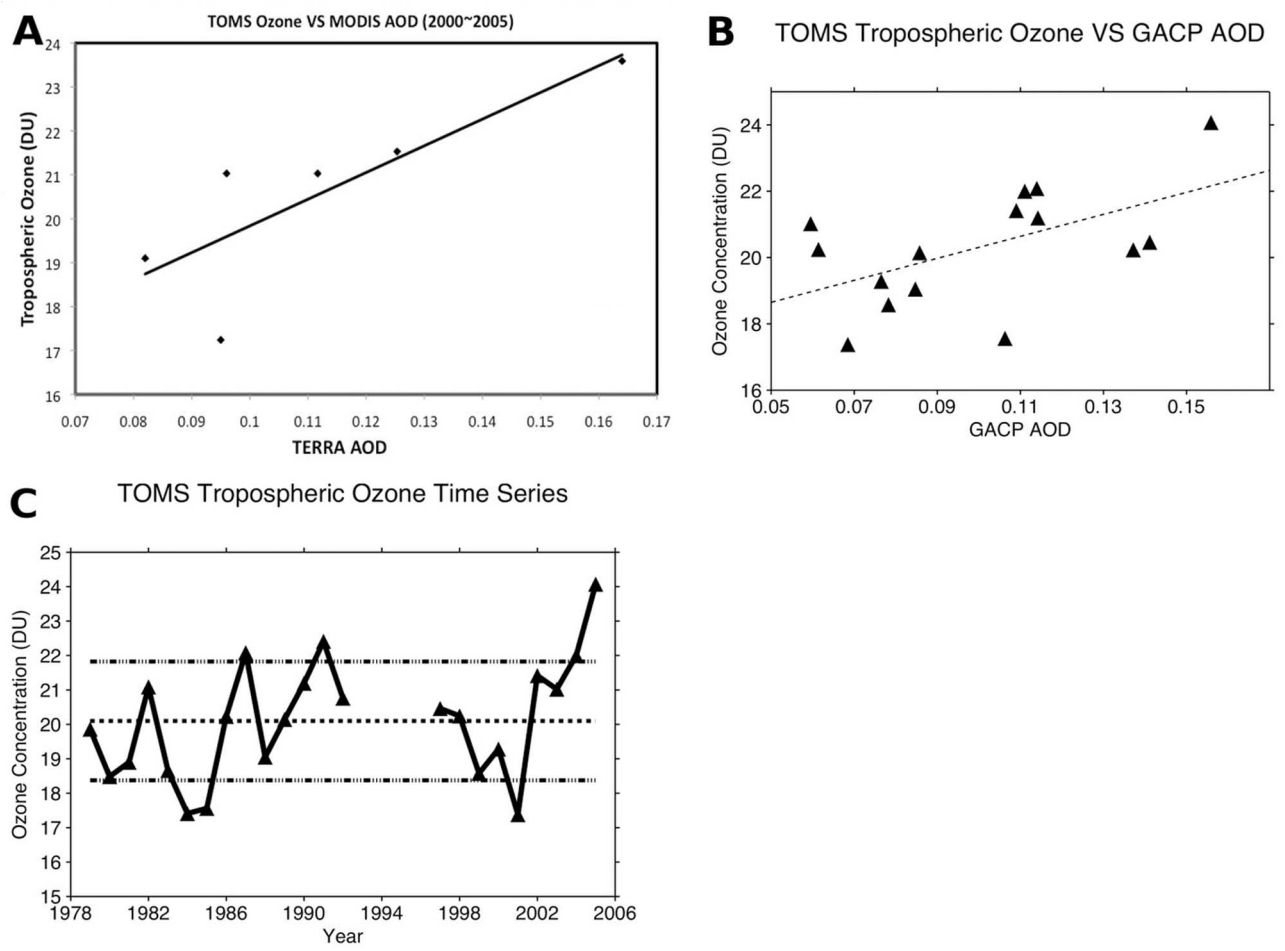

Figure 7. Correlations between (a) MODIS aerosol optical depth and (b) GACP aerosol optical depth and tropospheric ozone from TOMS. (c) Time series of TOMS tropospheric O_3 concentration for the past 27 years during the summer averaged over the region of interest. The dotted line is the climatological mean and the two dashed-dot lines are one standard deviation away from the mean.

previous modeling studies using different models seem to show different sensitivities of O_3 to lightning released NO_x [*Martin et al.*, 2002b; *Sauvage et al.*, 2007; *Wild*, 2007]). Further investigation on these fronts to improve our quantification of this sensitivity and its temporal and geographic distribution is needed, which is beyond the scope of this manuscript. Nevertheless, if we focus on the area west of 135°E where most lightning increase takes place, the ratios between O_3 anomaly and NO_2 anomaly are within a factor of 2 from satellite analysis and model results. Therefore, despite the quantitative difference the model results support the proposed aerosol-cloud-ozone chemistry link based on observations. This link represents a new indirect effect of aerosols on ozone chemistry via lightning and resultant LNO_x emissions.

3.5. Long-Term Perspective

[25] The relationship between aerosols and tropospheric ozone manifests itself not just in the anomaly seen in 2005 against the backdrop of the 5–10 year of "climatology." Figures 7a and 7b shows correlations between aerosol optical depth and TOMS tropospheric ozone using MODIS and GACP data, respectively, over the same region. The correlation coefficients for these two plots are significant at 95% ($r^2 = 0.67$) and 98% ($r^2 = 0.41$), respectively. In Figure 7b we exclude data from two 3-year periods (1982–1984 and 1991–1993) due to eruptions of El Chichon and Pinatubo. Sensitivity of tropospheric O_3 to aerosols, measured as DU per unit of aerosol optical depth, equals 60 and 30 in Figures 7a and 7b, respectively. If we focus on the MODIS period (2000–2005) the sensitivity based on GACP data gives the same sensitivity of 60 DU per aerosol optical depth. Both values, however, demonstrate the strong sensitivity of tropospheric O_3 concentration to changes in aerosol. This is in line with the strong sensitivity of lightning to aerosols and high efficiency of LNO_x in O_3 formation over clean regions. We find insignificant correlation between O_3 concentration and El Nino and Southern Oscillation indices for this particular region ($r = 0.38$, $p > 0.15$). Figure 7c provides a long-term perspective on the time evolution of tropospheric O_3 over the region (0°–15°N, 125°–150°E) for the last 27 years. Tropospheric O_3 in 2005 stands out as the all-time high and its value is more than two standard deviations above the climatological mean, implying a significant impact of the

aerosols on ozone through lightning or at least suggesting the aerosol-ozone link proposed here is consistent with the data we have. However, we also note some of the correlation might also be due to the effect of pollution on O_3 production as discussed in section 3.3.

3.6. Estimate of Global Impact

[26] We estimate the global impact of this aerosol-ozone connection with GMI model. Many previous studies have been carried out using different chemical transport models to understand the sensitivity of tropospheric ozone to lightning [e.g., *Lamarque et al.*, 1996; *Mickley et al.*, 2001; *Martin et al.*, 2002b; *Zhang et al.*, 2003; *Horowitz*, 2006; *Wild*, 2007; *Wu et al.*, 2007]. Here we utilize the quantitative relationship between aerosol loading and lightning flashes counts reported here and in *Altaratz et al.* [2010] to give an estimate of the aerosol induced tropospheric ozone change since 1850. For this we briefly review current and previous works. In this work and in *Yuan et al.* [2011] the focus is on a very clean region of the West Pacific. These studies, in this region, show convincing positive correlation between AOD and flash counts, through the range of AOD encountered in this situation. The AOD range spans approximately 0.05 to 0.25 for biweekly averages of AOD, 0.10 to 0.16 for seasonal averages, which is shown in *Yuan et al.* [2011, Figures 1c and 1d]. However, it is unreasonable to expect the increase of flash rate with aerosols to continue without limit. Indeed, flash rate is expected to decrease once an optimum aerosol concentration is met because further increase in droplet concentration will decrease collision efficiency between cloud hydrometeors and thus suppress charge separation and lightning flash rate. *Altaratz et al.* [2010] studied an area with a much wider AOD range than the present work and their results are consistent with the expectation that lightning flash counts reach a maximum, and then decrease with increasing AOD. The turning point of increase to decrease occurs at approximately AOD = 0.25. Furthermore, we note that aerosol types in *Yuan et al.* [2011] and *Altaratz et al.* [2010] are sulfate and smoke, respectively. These two studies are also over different surfaces, tropical ocean and tropical forest/savanna, respectively. Despite these differences, both studies show strong increase in flash rate with aerosol concentration when AOD is smaller than 0.25 or so. The similarity in the two studies thus encourages speculation toward a global estimate.

[27] We use the following scaling approach to conduct our sensitivity simulations and gauge the impact of aerosol induced lightning change on O_3:

$$L = 20 * L_o * (AOD - 0.05) \text{ when AOD is less than } 0.25;$$
$$L = L_{\max}(1 - (AOD - 0.25)/5) \text{ when AOD is greater than } 0.25.$$

L_o and $L_{\max}$ are local lightning flash rates when AOD is 0.05 and 0.25. We set L to L_o when AOD is less than 0.05. Therefore, 0.05 is the baseline aerosol optical depth. The threshold of 0.25 is roughly based on results from *Altaratz et al.* [2010]. Our scaling formula is a conservative estimate compared to the results from two studies. For example, we apply an increasing rate of 20 per unit of AOD when AOD is less than 0.25, which is smaller than both the average value of stippled areas in Figure 2d and what is reported in *Altaratz et al.* [2010]. Also, decreasing rate of lightning flash rate is such that it becomes 0 when AOD is equal to 5, i.e., the decreasing rate is about 5% of that for increasing rate, which is smaller than what is estimated from *Altaratz et al.* [2010]. This scaling is applied locally to individual grids while the meteorology is kept the same. With this approach, lightning changes will have strong spatial heterogeneity that highlights the sensitivity of lightning to aerosol loading, which is different from most previous works where lightning is perturbed by the same magnitude everywhere. However, this exercise only represents a sensitivity study with a few important limitations as discussed in Section 4. Also, the simulated impact would obviously depend strongly on the scaling formula adopted.

[28] Applying the proposed formula the aerosol differences between 1850 and 2005 (Figure 8a) are transformed into lightning changes (Figure 8b). Aerosol loading has for the most part increased substantially since 1850 with only a few exceptions like over Southern U.S. and Northern Argentina [*Bian et al.*, 2009, 2010]. Due to the nonlinear relationship between aerosol loading and flash rates, however, large increases in AOD do not automatically translate into strong increases in lightning (e.g., Northern China and India). Largest increase in lightning frequency occurs over biomass burning regions in the tropics because of the clean background and strong increase of biomass burning aerosols. Using the same 2005 meteorology and trace gas emission differences of column NO_2 and tropospheric O_3 between runs with 2005 and 1850 lightning are plotted in Figures 8c and 8d for the JJA season, respectively. Depending on location this experiment suggests a lightning induced change of O_3 by 1–2 DU, or 1–6%, and of NO_2 by 0–20%. Pronounced heterogeneity is noted for these lightning induced changes in O_3 and NO_2 fields. The most sensitive areas are places downwind of active lightning producing continents in the tropics such as the tropical East Pacific downwind of Central America, the South China Sea and southern Indian Ocean, and Central Atlantic downwind of central Africa. Lower concentration of background O_3 precursors, strong anthropogenic biomass burning and ample convection all contribute to large sensitivity of LNO_x to aerosol loading. The increases are particularly pronounced when changes within the upper troposphere (the layer between 200 mb and 400 mb) are considered (Figure 9). At this level, the sensitivity of O_3 to lightning can be seen throughout the tropics and is also nearly exclusively confined within the tropical belt, where the tropopause is higher. The magnitude of sensitivity at upper troposphere is higher than that of total column O_3.

[29] The sensitivity of ozone to aerosol concentrations via the nonlinear aerosol-lightning link is likely to have been greater in 1850 than 2005 due to lower anthropogenic emissions during the pre-industrial period. In another experiment, we estimate the sensitivity of the 1850 atmosphere to aerosol-induced lightning changes. We find that the sensitivity is almost doubled (Figure 10) while the overall structure of change is quite similar with the exception of the area downwind of Eastern U.S. The nonlinear dependence of ozone production rate on NO_x and other precursors is likely responsible for this. The 1850/2005 contrast is also illustrated in Figure 11 where we show the sensitivity of O_3 concentration to aerosol induced LNO_x in DJF using 1850 and 2005 emissions. When lightning perturbation is applied to 1850 emission, O_3 concentration is strongly increased due to

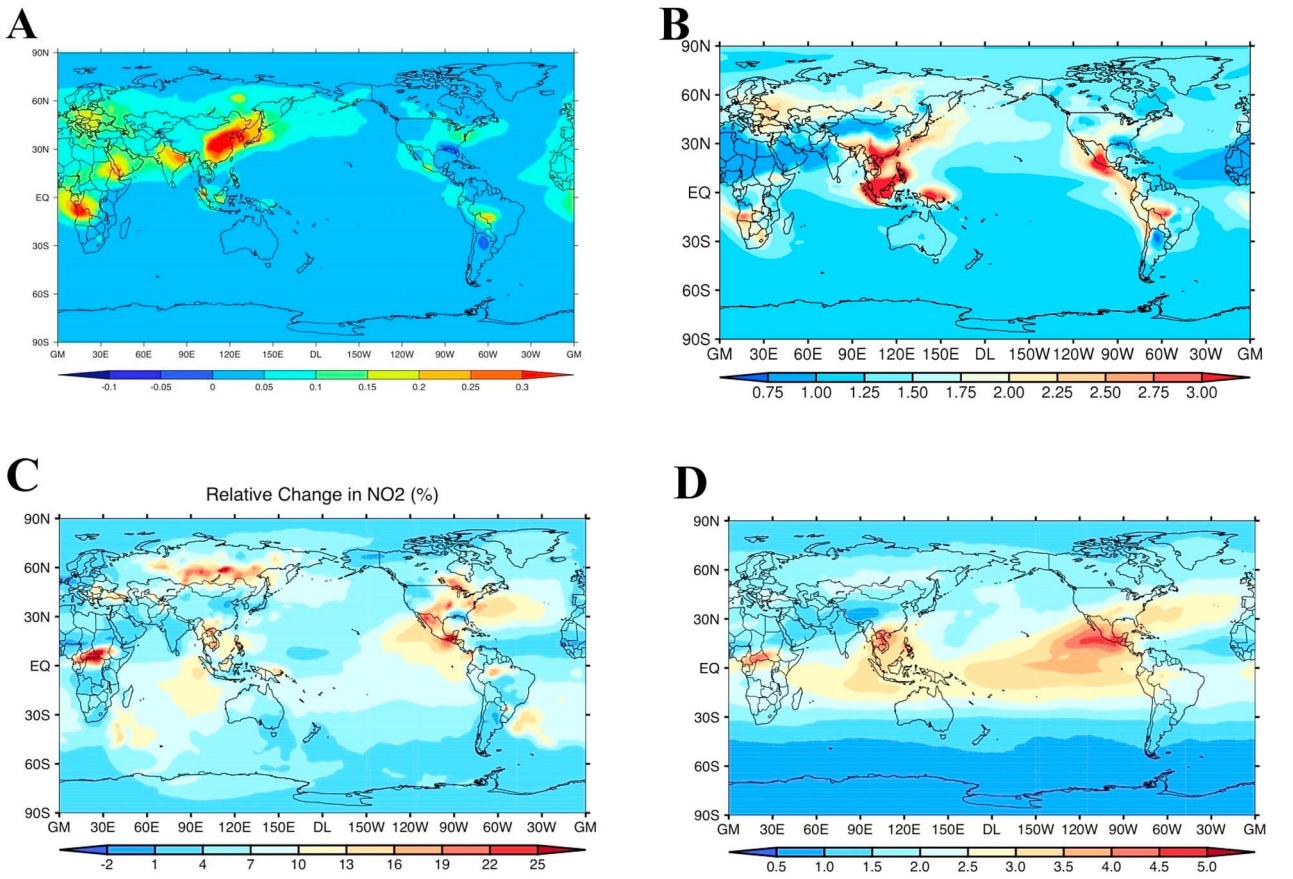

Figure 8. (a) JJA AOD difference between 2005 and 1850 based on GMI simulation. (b) Scaled lightning flash rate relative to 1850 in 2005. Except over Southeast U.S. and Northern Argentina lightning activity was lower due to cleaner air in 1850. (c) Relative change in tropospheric NO_2 resulting from the aerosol induced lightning change. (d) Same as Figure 8c, but for tropospheric O_3. The 2005 emission is used for this simulation.

increase of biomass burning aerosol induced LNO_x increase over the Indian Ocean downwind of western Indonesia. In the 2005 emission scenario, this area shows limited sensitivity because biomass burning introduced ozone precursor damps the dependence of O_3 production rate on LNO_x. The NO production of lightning changes resulting from the sensitivity simulations are shown in Table 3.

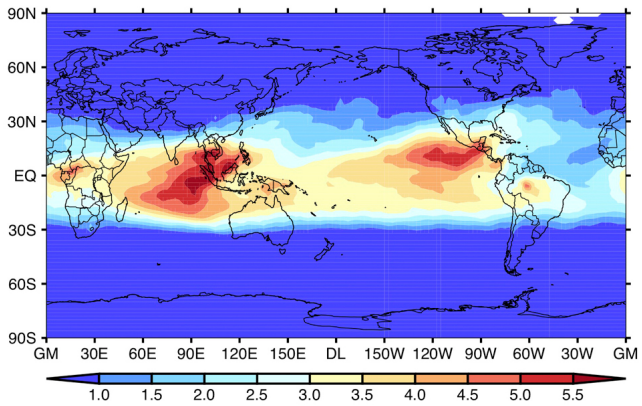

Figure 9. Same as Figures 8c or 8d, but for tropospheric O_3 in the layer between 200 mb and 400 mb.

4. Discussion and Implication

[30] The results of this study demonstrate a potentially important impact of aerosols on lightning and tropospheric ozone production. A quantitative global estimate of the

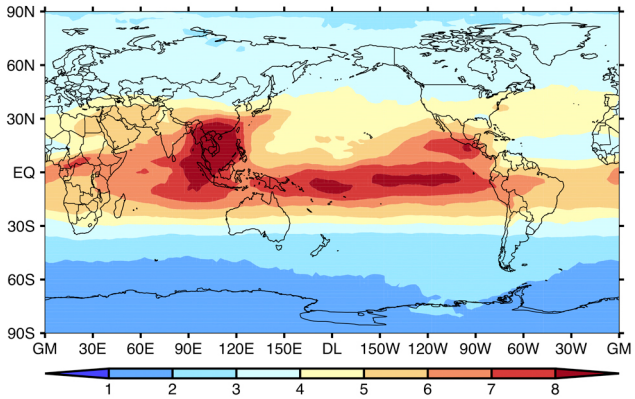

Figure 10. Similar to Figure 8d. In this case 1850 emission scenario is used instead of 2005. Due to the lower background emission the sensitivity of model fields to aerosol-induced perturbation is roughly doubled.

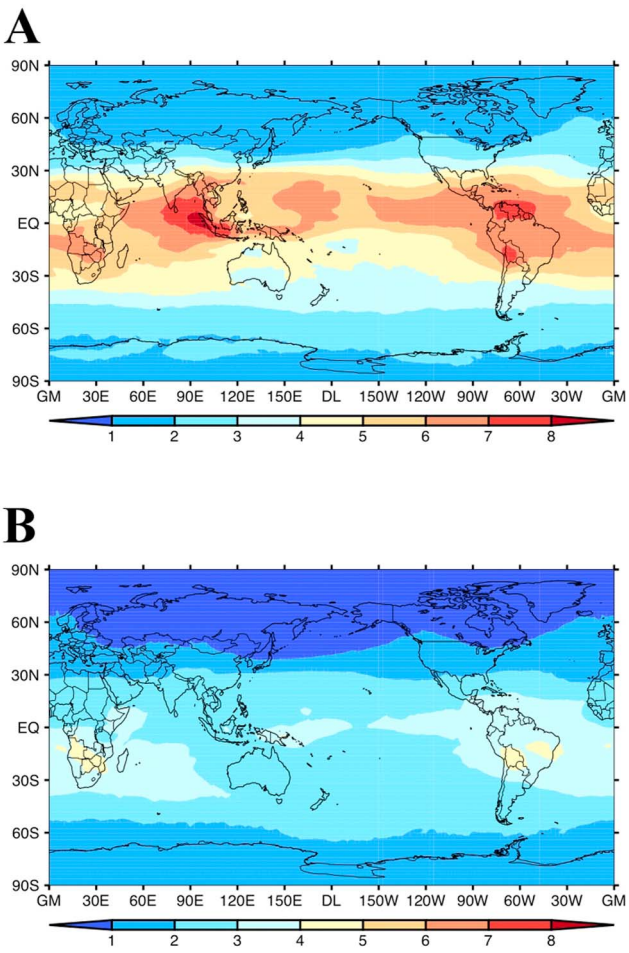

Figure 11. A further illustration of emission background dependence of aerosol effect on O_3. These two maps are for December, January and February. (a) 1850 emission, and (b) 2005. Beside the overall higher sensitivity (Figure 11a compared to Figure 11b) the main feature over Indian Ocean (Figure 11a) is completely missing in Figure 11b, reflecting the nonlinearity and competing direct and indirect effects of biomass burning on O_3.

aerosol indirect effect on tropospheric ozone concentration, however, faces further challenges and uncertainties. For example, the background conditions such as aerosol type and concentration as well as background meteorology could affect how aerosols affect convective clouds [*Fan et al.*, 2009]. Because of this the formula proposed here may not hold everywhere. Moreover, tropospheric ozone concentration is controlled by a set of nonlinear complex processes such as cloud radiative effects, photochemistry, convective transport and stratosphere-troposphere exchange. These processes may alter the details of aerosol-O_3 link demonstrated here. For example, the radiative effect of aerosol and cloud condensate can have an impact on the ozone related chemistry as shown by many studies [e.g., *Wang and Prinn*, 2000; *Martin et al.*, 2003; *Barth et al.*, 2007]. Furthermore, because both aerosol and O_3 have relatively short lifetimes and the aerosol effect on clouds depend on background environmental conditions we expect the effect aerosols on O_3 to be highly heterogeneous both in space and time. These complexities will require more advanced models and further observational studies to better quantify the processes at work and project global consequences. For example, compared to previous modeling results, the ratio of O_3 to NO_2 change reported here is smaller. As discussed above, this ratio may be model dependent because of many physical and chemical processes are modeled differently. Further investigations and comparisons are needed to elucidate the model difference and to improve our understanding. Finally, the change in O_3 will affect characteristics of other chemical trace gases and species such as methane and carbon monoxide etc., which will require a coupled chemistry-climate model to understand these interactions.

[31] Nevertheless, the aerosol effect on O_3 via lightning demonstrated here opens up a new set of possibilities for aerosol, O_3 and lightning studies (Figure 12). For example, the aerosol-lightning-ozone link offers a physical mechanism that may account for a part of the difference between modeled and observed background O_3 in the later 19th century [*Marenco et al.*, 1994], which is however dependent on shape of the vertical profile of LNO_x. Surface concentrations should not change by more than a few ppbv and a considerable bias is likely to remain given our current understanding of the vertical profile of LNO_x. The proposed aerosol-lightning-ozone link would have its strongest impact in the mid- and upper-troposphere. The link implies lower LNO_x source strength in the 19th century [*Mickley et al.*, 2001] given the lower aerosol concentration, which would mean a substantially lower upper tropospheric O_3 concentration in preindustrial era. This would imply a larger tropospheric O_3 radiative forcing than current estimate [*Mickley et al.*, 2001; *Shindell et al.*, 2003], e.g., 0.5 Wm^{-2} larger according to [*Mickley et al.*, 2001]. Interestingly, the stronger ozone forcing would improve agreement between model and observed climate change in the 20th century [*Shindell et al.*, 2006]. Due to the vertical distribution of LNO_x its impact on tropospheric ozone may have a strong influence on mid-to-upper troposphere O_3 production [*Pickering et al.*, 1998; *Ott et al.*, 2010] although curiously, stronger thunderstorms (e.g., invigorated by aerosols) in the midlatitudes might induce ozone loss in the lower-stratosphere due to injection of water vapor there [*Anderson et al.*, 2012]. As implied by our sensitivity simulations, aerosol introduced O_3 change may not be well detected by historical observations because its major influence is over remote oceanic areas and within the upper troposphere. In addition, anthropogenic emissions are undergoing a profound change: decreasing in the midlatitudes (with the exception of Northeast Asia where trends are unclear) and increasing in the

Table 3. The Total NO Productions From Lightning From Two Seasons Shown Using 2005 Emission[a]

Summer (TgNO/month)	July	August	September
Control	0.73	0.66	0.72
Adj	0.50	0.44	0.48
Winter (TgNO/month)	**December**	**January**	**Feburary**
Control	0.39	0.50	0.36
Adj	0.27	0.35	0.25

[a]Numbers in the 'adj' rows refer to lightning NO production when 1850 AOD values are used to scale the lightning.

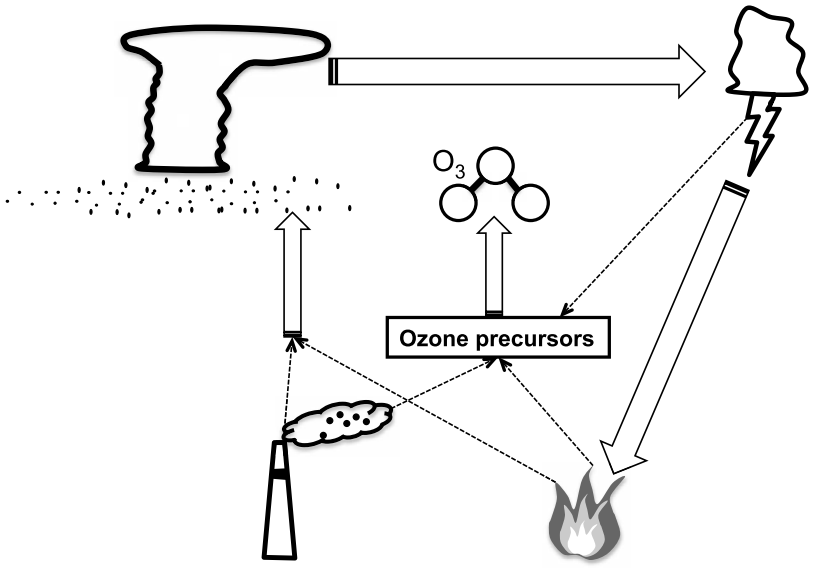

Figure 12. A conceptual diagram of how anthropogenic aerosols and emissions directly and indirectly affect tropospheric O_3. The indirect pathway is through aerosol impacting deep convective cloud properties and lightning activity, which leads to LNO_x perturbation and therefore tropospheric O_3 production. The feedback link between lightning and fire activity over the higher latitude boreal forest region warrants further investigation.

lower latitudes [*Shindell et al.*, 2006; *Lamarque et al.*, 2010]. As emissions shift equator-ward, anthropogenic aerosols may strongly affect tropical convective clouds, enhance LNO_X production as well as NO_x from other sources and result in more tropospheric O_3 [*Lelieveld and Dentener*, 2000; *Lelieveld et al.*, 2004; *Yuan et al.*, 2011]. The aerosol effect on O_3 is a positive component to the overall negative aerosol radiative forcing and the intricate aerosol-cloud-chemistry interactions make it imperative to study them with an integrated approach in our climate system.

[32] The aerosol-lightning-ozone connection for maritime convection may also be valuable for understanding ozone long-range transport and the O_3 trend in relatively clean regions [*Cooper et al.*, 2010; *Lelieveld et al.*, 2004]. Over the North Pacific, for example, studies have shown that storm track clouds are invigorated by outflow of Asian pollution aerosols in recent decades [*Zhang et al.*, 2007]. Given the high sensitivity of lightning and LNO_x to aerosol input over maritime convective clouds, it could be speculated that the anthropogenic increase of aerosol influx into the North Pacific region could have contributed to increase of tropospheric ozone production and transport to the west coast of North America [*Zhang et al.*, 2008]. Aerosol increase introduced by biomass burning of tropical and boreal forests in the last decades may also impact convection and lightning activity. However, it will be challenging to untangle the direct effect and indirect effect (through aerosol-lightning-ozone) of biomass burning on tropospheric ozone production since both are positive effects. It probably could only be solved through model simulations with appropriate physical and chemical processes. Over the higher-latitude boreal forest area, we note a potential positive feedback between fire activity and aerosol concentration. Increased aerosol loading (initiated by pollution and/or climate change induced fire activity [*Flannigan et al.*, 2005] enhances the chance of lightning, which in turn increases fire activity and biomass burning aerosol concentration (Figures 8c and 12). This is a potentially strong feedback loop because dry thunderstorms (thunderstorms without or with little precipitation) are the major source of ignition for wild boreal forest fires [*Flannigan et al.*, 2005]. Both precipitation suppression and lightning enhancing effects of aerosols work to increase fire activity. This positive feedback can have important impact on atmosphere chemistry and forest ecosystem in high latitude regions.

[33] We summarize this paper with a conceptual diagram in Figure 12. Increase of aerosol concentration within convective clouds modifies cloud microphysical processes and invigorates convection. This in-turn enhances lightning activity and increases LNO_x release into the atmosphere, especially in the clean upper troposphere, which generally favors tropospheric O_3 production. Over the boreal forest aerosol-induced dry thunderstorms can positively feedback to fire ignition and biomass burning aerosol production, which increases ozone precursors among other impacts on atmospheric chemistry. These integrated aerosol-cloud-chemistry interactions demand more investigations to fully characterize its impact.

5. Summary and Conclusion

[34] We demonstrate an aerosol indirect effect on atmosphere chemistry, particularly tropospheric ozone, by affecting convective cloud lightning activity. Strong sensitivity of lightning flash rate, on the order of around 30-fold increase per unit of aerosol optical depth, leads to significant release of LNO_x, which increases tropospheric ozone production, especially in the upper troposphere. Careful analyses are carried out to examine and reject alternative hypotheses. Model simulations corroborate the aerosol-lightning-ozone

link demonstrated by satellite data analyses. Long-term satellite measurements show a significant correlation between aerosol concentration and tropospheric ozone concentration, lending further support for the hypothesized link. This link is currently not considered in global models and preliminary model sensitivity experiments indicate it has important implications for understanding past and projecting future tropospheric ozone forcing changes. This link also implies a potential positive feedback between boreal forest fire and lightning. The potential of and the challenge of characterizing this aerosol-lightning-ozone link are discussed.

[35] **Acknowledgment.** We thank three anonymous reviewers for their constructive suggestions to improve our manuscript. We acknowledge the free use of tropospheric NO_2 column data from the various groups including OMI, GOME, SCIAMARCHY from www.temis.nl; Randall Martin's group from http://fizz.phys.dal.ca/~atmos/g47.swf; and the University of Bremen group from http://www.iup.uni-bremen.de/doas/index.html . The LIS data set and associated analysis were in part supported by the NASA Earth Observing System, the TRMM Lightning Imaging Sensor Instrument team, and the NOAA GOES-R Geostationary Lightning Mapper science team. The LIS data are available from the NASA EOSDIS Global Hydrology Resource Center DAAC, Huntsville, Alabama, USA, http://thunder.nsstc.nasa.gov. We would also acknowledge funding support for this work by NASA's IDS and Radiation Science programs.

References

Albrecht, R., C. Morales, and M. Dias (2011), Electrification of precipitating systems over the Amazon: Physical processes of thunderstorm development, *J. Geophys. Res.*, *116*, D08209, doi:10.1029/2010JD014756.

Allen, D. J., and K. E. Pickering (2002), Evaluation of lightning flash rate parameterizations for use in a global chemical transport model, *J. Geophys. Res.*, *107*(D23), 4711, doi:10.1029/2002JD002066.

Allen, D., K. Pickering, B. Duncan, and M. Damon (2010), Impact of lightning NO emissions on North American photochemistry as determined using the Global Modeling Initiative (GMI) model, *J. Geophys. Res.*, *115*, D22301, doi:10.1029/2010JD014062.

Altaratz, O., I. Koren, Y. Yair, and C. Price (2010), Lightning response to smoke from Amazonian fires, *Geophys. Res. Lett.*, *37*, L07801, doi:10.1029/2010GL042679.

Anderson, J. G., D. M. Wilmouth, J. B. Smith, and D. S. Sayres (2012), UV dosage levels in summer: Increased risk of ozone loss from convectively injected water vapor, *Science*, *337*, 835–839, doi:10.1126/science.1222978.

Barth, M. C., et al. (2007), Cloud-scale model intercomparison of chemical constituent transport in deep convection, *Atmos. Chem. Phys.*, *7*(18), 4709–4731, doi:10.5194/acp-7-4709-2007.

Beirle, S., H. Huntrieser, and T. Wagner (2010), Direct satellite observation of lightning-produced NOx, *Atmos. Chem. Phys.*, *10*(22), 10,965–10,986, doi:10.5194/acp-10-10965-2010.

Bian, H. S., and M. Prather (2002), Fast-J2: Accurate simulation of stratospheric photolysis in global chemical models, *J. Atmos. Chem.*, *41*(3), 281–296, doi:10.1023/A:1014980619462.

Bian, H., M. Chin, J. M. Rodriguez, H. Yu, J. Penner, and S. E. Strahan (2009), Sensitivity of aerosol optical thickness and aerosol direct radiative effect to relative humidity, *Atmos. Chem. Phys.*, *9*, 2375–2386, doi:10.5194/acp-9-2375-2009.

Bian, H., M. Chin, S. Kawa, H. Yu, T. Diehl, and T. Kucsera (2010), Multiscale carbon monoxide and aerosol correlations from satellite measurements and the GOCART model: Implication for emissions and atmospheric evolution, *J. Geophys. Res.*, *115*, D07302, doi:10.1029/2009JD012781.

Boccippio, D. J., W. J. Koshak, and R. J. Blakeslee (2002), Performance assessment of the optical transient detector and lightning Imaging sensor. Part I: Predicted diurnal variability, *J. Atmos. Oceanic Technol.*, *19*(9), 1318–1332, doi:10.1175/1520-0426(2002)019<1318:PAOTOT>2.0.CO;2.

Boersma, K., H. Eskes, and E. Brinksma (2004), Error analysis for tropospheric NO_2 retrieval from space, *J. Geophys. Res.*, *109*, D04311, doi:10.1029/2003JD003962.

Boersma, K., et al. (2007), Near-real time retrieval of tropospheric NO2 from OMI, *Atmos. Chem. Phys.*, *7*(8), 2103–2118, doi:10.5194/acp-7-2103-2007.

Boersma, K. F., et al. (2008), Validation of OMI tropospheric NO_2 observations during INTEX-B and application to constrain NOx emissions over the eastern United States and Mexico, *Atmos. Environ.*, *42*(19), 4480–4497, doi:10.1016/j.atmosenv.2008.02.004.

Bojkov, R. (1986), Surface ozone during the 2nd-half of the 19th-century, *J. Clim. Appl. Meteorol.*, *25*(3), 343–352, doi:10.1175/1520-0450(1986)025<0343:SODTSH>2.0.CO;2.

Bucsela, E., E. Celarier, M. Wenig, J. Gleason, J. Veefkind, K. Boersma, and E. Brinksma (2006), Algorithm for NO_2 vertical column retrieval from the ozone monitoring instrument, *IEEE Trans. Geosci. Remote*, *44*(5), 1245–1258, doi:10.1109/TGRS.2005.863715.

Bucsela, E. J., et al. (2010), Lightning-generated NOx seen by the Ozone Monitoring Instrument during NASA's Tropical Composition, Cloud and Climate Coupling Experiment (TC4), *J. Geophys. Res.*, *115*, D00J10, doi:10.1029/2009JD013118.

Chin, M., T. Diehl, O. Dubovik, T. F. Eck, B. Holben, A. Sinyuk, and D. G. Streets (2009), Light absorption by pollution, dust and biomass burning aerosols: A global model study and evaluation with AERONET data, *Ann. Geophys.*, *27*, 3439–3464, doi:10.5194/angeo-27-3439-2009.

Christian, H. J., et al. (2003), Global frequency and distribution of lightning as observed from space by the Optical Transient Detector, *J. Geophys. Res.*, *108*(D1), 4005, doi:10.1029/2002JD002347.

Chronis, T., S. Goodman, D. Cecil, D. Buechler, F. Robertson, J. Pittman, and R. Blakeslee (2008), Global lightning activity from the ENSO perspective, *Geophys. Res. Lett.*, *35*, L19804, doi:10.1029/2008GL034321.

Cooper, O. R., et al. (2006), Large upper tropospheric ozone enhancements above midlatitude North America during summer: In situ evidence from the IONS and MOZAIC ozone measurement network, *J. Geophys. Res.*, *111*, D24S05, doi:10.1029/2006JD007306.

Cooper, O. R., et al. (2010), Increasing springtime ozone mixing ratios in the free troposphere over western North America, *Nature*, *463*(7279), 344–348, doi:10.1038/nature08708.

Duncan, B., S. Strahan, Y. Yoshida, S. Steenrod, and N. Livesey (2007), Model study of the cross-tropopause transport of biomass burning pollution, *Atmos. Chem. Phys.*, *7*(14), 3713–3736, doi:10.5194/acp-7-3713-2007.

Duncan, B., J. J. West, Y. Yoshida, A. M. Fiore, and J. Ziemke (2008), The influence of European pollution on ozone in the Near East and northern Africa, *Atmos. Chem. Phys.*, *8*, 2267–2283, doi:10.5194/acp-8-2267-2008.

Edwards, D. P., et al. (2003), Tropospheric ozone over the tropical Atlantic: A satellite perspective, *J. Geophys. Res.*, *108*(D8), 4237, doi:10.1029/2002JD002927.

Fan, J., T. Yuan, J. M. Comstock, S. Ghan, A. Khain, L. R. Leung, Z. Li, V. J. Martins, and M. Ovchinnikov (2009), Dominant role by vertical wind shear in regulating aerosol effects on deep convective clouds, *J. Geophys. Res.*, *114*, D22206, doi:10.1029/2009JD012352.

Flannigan, M., K. Logan, B. Amiro, W. Skinner, and B. Stocks (2005), Future area burned in Canada, *Clim. Change*, *72*(1–2), 1–16, doi:10.1007/s10584-005-5935-y.

Gauss, M., et al. (2006), Radiative forcing since preindustrial times due to ozone change in the troposphere and the lower stratosphere, *Atmos. Chem. Phys.*, *6*, 575–599, doi:10.5194/acp-6-575-2006.

Geogdzhayev, I., M. Mishchenko, E. Terez, G. Terez, and G. Gushchin (2005), Regional advanced very high resolution radiometer-derived climatology of aerosol optical thickness and size, *J. Geophys. Res.*, *110*, D23205, doi:10.1029/2005JD006170.

Goodman, S., D. Buechler, K. Knupp, K. Driscoll, and E. Mccaul (2000), The 1997–98 El Nino event and related wintertime lightning variations in the southeastern United States, *Geophys. Res. Lett.*, *27*(4), 541–544, doi:10.1029/1999GL010808.

Goodman, S., D. E. Buechler, and E. Mccaul (2007), Lightning, in *Our Changing Planet: The View From Space*, pp. 44–52, Cambridge Univ. Press, Cambridge, U. K.

Guenther, A., et al. (1995), A global-model of natural volatile organic compound emissions, *J. Geophys. Res.*, *100*, 8873–8892, doi:10.1029/94JD02950.

Guenther, A., T. Karl, P. Harley, C. Wiedinmyer, P. I. Palmer, and C. Geron (2006), Estimates of global terrestrial isoprene emissions using MEGAN (Model of Emissions of Gases and Aerosols from Nature), *Atmos. Chem. Phys.*, *6*, 3181–3210, doi:10.5194/acp-6-3181-2006.

Hauglustaine, D. A., and G. P. Brasseur (2001), Evolution of tropospheric ozone under anthropogenic activities and associated radiative forcing of climate, *J. Geophys. Res.*, *106*(D23), 32,337–32,360, doi:10.1029/2001JD900175.

Hauglustaine, D., L. Emmons, M. Newchurch, G. Brasseur, T. Takao, K. Matsubara, J. Johnson, B. Ridley, J. Stith, and J. Dye (2001), On the role of lightning NOx in the formation of tropospheric ozone plumes: A global model perspective, *J. Atmos. Chem.*, *38*(3), 277–294, doi:10.1023/A:1006452309388.

Horowitz, L. W. (2006), Past, present, and future concentrations of tropospheric ozone and aerosols: Methodology, ozone evaluation, and sensitivity to aerosol wet removal, *J. Geophys. Res.*, *111*, D22211, doi:10.1029/2005JD006937.

Jacobson, M. (1995), Computation of global photochemistry with SMVGEAR-II, *Atmos. Environ.*, *29*(18), 2541–2546, doi:10.1016/1352-2310(95)00194-4.

Labrador, L., R. von Kuhlmann, and M. Lawrence (2005), The effects of lightning-produced NOx and its vertical distribution on atmospheric chemistry: Sensitivity simulations with MATCH-MPIC, *Atmos. Chem. Phys.*, *5*, 1815–1834, doi:10.5194/acp-5-1815-2005.

Lamarque, J. F., G. P. Brasseur, and P. G. Hess (1996), Three-dimensional study of the relative contributions of the different nitrogen sources in the troposphere, *J. Geophys. Res.*, *101*(D17), 22,955–22,968, doi:10.1029/96JD02160.

Lamarque, J. F., P. Hess, L. Emmons, L. Buja, W. Washington, and C. Granier (2005), Tropospheric ozone evolution between 1890 and 1990, *J. Geophys. Res.*, *110*, D08304, doi:10.1029/2004JD005537.

Lamarque, J., et al. (2010), Historical (1850–2000) gridded anthropogenic and biomass burning emissions of reactive gases and aerosols: Methodology and application, *Atmos. Chem. Phys.*, *10*(15), 7017–7039, doi:10.5194/acp-10-7017-2010.

Lelieveld, J., and F. J. Dentener (2000), What controls tropospheric ozone?, *J. Geophys. Res.*, *105*(D3), 3531–3551, doi:10.1029/1999JD901011.

Lelieveld, J., J. Van Aardenne, H. Fischer, M. De Reus, J. Williams, and P. Winkler (2004), Increasing ozone over the Atlantic Ocean, *Science*, *304*(5676), 1483–1487, doi:10.1126/science.1096777.

Logan, J. A. (1985), Tropospheric ozone: Seasonal behavior, trends, and anthropogenic influence, *J. Geophys. Res.*, *90*(D6), 10,463–10,482, doi:10.1029/JD090iD06p10463.

Lyons, W. A., T. E. Nelson, E. R. Williams, J. A. Cramer, and T. R. Turner (1998), Enhanced positive cloud-to-ground lightning in thunderstorms ingesting smoke from fires, *Science*, *282*(5386), 77–80, doi:10.1126/science.282.5386.77.

Marenco, A., H. Gouget, P. Nedelec, J. Pages, and F. Karcher (1994), Evidence of a long-term increase in tropospheric ozone from Pic Du Midi data series- consequences- positive radiative forcing, *J. Geophys. Res.*, *99*(D8), 16,617–16,632, doi:10.1029/94JD00021.

Martin, R. V., et al. (2002a), An improved retrieval of tropospheric nitrogen dioxide from GOME, *J. Geophys. Res.*, *107*(D20), 4437, doi:10.1029/2001JD001027.

Martin, R. V., et al. (2002b), Interpretation of TOMS observations of tropical tropospheric ozone with a global model and in situ observations, *J. Geophys. Res.*, *107*(D18), 4351, doi:10.1029/2001JD001480.

Martin, R. V., D. J. Jacob, R. M. Yantosca, M. Chin, and P. Ginoux (2003), Global and regional decreases in tropospheric oxidants from photochemical effects of aerosols, *J. Geophys. Res.*, *108*(D3), 4097, doi:10.1029/2002JD002622.

Martin, R., C. Sioris, K. Chance, T. Ryerson, T. Bertram, P. Wooldridge, R. Cohen, J. Neuman, A. Swanson, and F. Flocke (2006), Evaluation of space-based constraints on global nitrogen oxide emissions with regional aircraft measurements over and downwind of eastern North America, *J. Geophys. Res.*, *111*, D15308, doi:10.1029/2005JD006680.

Martin, R. V., B. Sauvage, I. Folkins, C. E. Sioris, C. Boone, P. Bernath, and J. Ziemke (2007), Space-based constraints on the production of nitric oxide by lightning, *J. Geophys. Res.*, *112*, D09309, doi:10.1029/2006JD007831.

Mickley, L. J., D. J. Jacob, and D. Rind (2001), Uncertainty in preindustrial abundance of tropospheric ozone: Implications for radiative forcing calculations, *J. Geophys. Res.*, *106*(D4), 3389–3399, doi:10.1029/2000JD900594.

Morris, G., A. Thompson, K. Pickering, S. Chen, E. Bucsela, and P. Kucera (2010), Observations of ozone production in a dissipating tropical convective cell during TC4, *Atmos. Chem. Phys.*, *10*(22), 11,189–11,208, doi:10.5194/acp-10-11189-2010.

Oltmans, S. J., et al. (2006), Long-term changes in tropospheric ozone, *Atmos. Environ.*, *40*(17), 3156–3173, doi:10.1016/j.atmosenv.2006.01.029.

Ott, L., K. Pickering, G. Stenchikov, D. Allen, A. Decaria, B. Ridley, R. Lin, S. Lang, and W. Tao (2010), Production of lightning NOx and its vertical distribution calculated from three-dimensional cloud-scale chemical transport model simulations, *J. Geophys. Res.*, *115*, D04301, doi:10.1029/2009JD011880.

Pickering, K. E., Y. S. Wang, W. K. Tao, C. Price, and J. F. Muller (1998), Vertical distributions of lightning NOx for use in regional and global chemical transport models, *J. Geophys. Res.*, *103*(D23), 31,203–31,216, doi:10.1029/98JD02651.

Remer, L. A., et al. (2005), The MODIS aerosol algorithm, products, and validation, *J. Atmos. Sci.*, *62*(4), 947–973, doi:10.1175/JAS3385.1.

Richter, A., and J. Burrows (2002), Tropospheric NO_2 from GOME measurements, *Adv. Space Res.*, *29*(11), 1673–1683.

Sauvage, B., R. V. Martin, A. Van Donkelaar, and J. R. Ziemke (2007), Quantification of the factors controlling tropical tropospheric ozone and the South Atlantic maximum, *J. Geophys. Res.*, *112*, D11309, doi:10.1029/2006JD008008.

Schumann, U., and H. Huntrieser (2007), The global lightning-induced nitrogen oxides source, *Atmos. Chem. Phys.*, *7*(14), 3823–3907, doi:10.5194/acp-7-3823-2007.

Sherwood, S. C., V. T. J. Phillips, and J. S. Wettlaufer (2006), Small ice crystals and the climatology of lightning, *Geophys. Res. Lett.*, *33*, L05804, doi:10.1029/2005GL025242.

Shindell, D. T., G. Faluvegi, and N. Bell (2003), Preindustrial-to-present-day radiative forcing by tropospheric ozone from improved simulations with the GISS chemistry-climate GCM, *Atmos. Chem. Phys.*, *3*, 1675–1702, doi:10.5194/acp-3-1675-2003.

Shindell, D., G. Faluvegi, A. Lacis, J. Hansen, R. Ruedy, and E. Aguilar (2006), Role of tropospheric ozone increases in 20th-century climate change, *J. Geophys. Res.*, *111*, D08302, doi:10.1029/2005JD006348.

Solomon, S., D. W. J. Thompson, R. W. Portmann, S. J. Oltmans, and A. M. Thompson (2005), On the distribution and variability of ozone in the tropical upper troposphere: Implications for tropical deep convection and chemical-dynamical coupling, *Geophys. Res. Lett.*, *32*, L23813, doi:10.1029/2005GL024323.

Solomon, S., et al. (2007), *Climate Change 2007: The Physical Science Basis: Contribution of Working Group I to the Fourth Assessment Report of the Intergovernmental Panel on Climate Change*, Cambridge Univ. Press, New York.

Stevenson, D. S., et al. (2006), Multimodel ensemble simulations of present-day and near-future tropospheric ozone, *J. Geophys. Res.*, *111*, D08301, doi:10.1029/2005JD006338.

Thompson, A. M. (1992), THE oxidizing capacity of the Earth's atmosphere-probable past and future changes, *Science*, *256*(5060), 1157–1165, doi:10.1126/science.256.5060.1157.

Thompson, A. M., B. G. Doddridge, J. C. Witte, R. D. Hudson, W. T. Luke, J. E. Johnston, B. J. Johnston, S. J. Oltmans, and R. Weller (2000), A tropical Atlantic paradox: Shipboard and satellite views of a tropospheric ozone maximum and wave-one in January-February 1999, *Geophys. Res. Lett.*, *27*(20), 3317–3320, doi:10.1029/1999GL011273.

Thompson, A. M., et al. (2003), Southern Hemisphere Additional Ozonesondes (SHADOZ) 1998–2000 tropical ozone climatology: 2. Tropospheric variability and the zonal wave-one, *J. Geophys. Res.*, *108*(D2), 8241, doi:10.1029/2002JD002241.

Tie, X. X., R. Y. Zhang, G. Brasseur, L. Emmons, and W. F. Lei (2001), Effects of lightning on reactive nitrogen and nitrogen reservoir species in the troposphere, *J. Geophys. Res.*, *106*(D3), 3167–3178, doi:10.1029/2000JD900565.

Tie, X. X., S. Madronich, S. Walters, R. Y. Zhang, P. Rasch, and W. Collins (2003), Effect of clouds on photolysis and oxidants in the troposphere, *J. Geophys. Res.*, *108*(D20), 4642, doi:10.1029/2003JD003659.

Volz, A., and D. Kley (1988), Evaluation of the Montsouris series of ozone measurements made in the 19th century, *Nature*, *332*(6161), 240–242, doi:10.1038/332240a0.

Voulgarakis, A., O. Wild, N. H. Savage, G. D. Carver, and J. A. Pyle (2009), Clouds, photolysis and regional tropospheric ozone budgets, *Atmos. Chem. Phys.*, *9*(21), 8235–8246, doi:10.5194/acp-9-8235-2009.

Wang, C., and R. Prinn (2000), On the roles of deep convective clouds in tropospheric chemistry, *J. Geophys. Res.*, *105*(D17), 22,269–22,297, doi:10.1029/2000JD900263.

Wang, Y. H., and D. J. Jacob (1998), Anthropogenic forcing on tropospheric ozone and OH since preindustrial times, *J. Geophys. Res.*, *103*(D23), 31,123–31,135, doi:10.1029/1998JD100004.

Wild, O. (2007), Modelling the global tropospheric ozone budget: Exploring the variability in current models, *Atmos. Chem. Phys.*, *7*(10), 2643–2660, doi:10.5194/acp-7-2643-2007.

Wild, O., X. Zhu, and M. Prather (2000), Fast-j: Accurate simulation of in- and below-cloud photolysis in tropospheric chemical models, *J. Atmos. Chem.*, *37*(3), 245–282, doi:10.1023/A:1006415919030.

Williams, E. R. (2005), Lightning and climate: A review, *Atmos. Res.*, *76*(1–4), 272–287, doi:10.1016/j.atmosres.2004.11.014.

Williams, E., and S. Stanfill (2002), The physical origin of the land-ocean contrast in lightning activity, *C. R. Phys.*, *3*(10), 1277–1292, doi:10.1016/S1631-0705(02)01407-X.

Williams, E., et al. (2002), Contrasting convective regimes over the Amazon: Implications for cloud electrification, *J. Geophys. Res.*, *107*(D20), 8082, doi:10.1029/2001JD000380.

Wu, S., L. J. Mickley, D. J. Jacob, J. A. Logan, R. M. Yantosca, and D. Rind (2007), Why are there large differences between models in global

budgets of tropospheric ozone?, *J. Geophys. Res.*, *112*, D05302, doi:10.1029/2006JD007801.

Yuan, T., and Z. Li (2010), General macro- and microphysical properties of deep convective clouds as observed by MODIS, *J. Clim.*, *23*, 3457–3473.

Yuan, T., J. V. Martins, Z. Li, and L. A. Remer (2010), Estimating glaciation temperature of deep convective clouds with remote sensing data, *Geophys. Res. Lett.*, *37*, L08808, doi:10.1029/2010GL042753.

Yuan, T., L. A. Remer, K. E. Pickering, and H. Yu (2011), Observational evidence of aerosol enhancement of lightning activity and convective invigoration, *Geophys. Res. Lett.*, *38*, L04701, doi:10.1029/2010GL046052.

Zhang, L., et al. (2008), Transpacific transport of ozone pollution and the effect of recent Asian emission increases on air quality in North America: An integrated analysis using satellite, aircraft, ozonesonde, and surface observations, *Atmos. Chem. Phys.*, *8*(20), 6117–6136, doi:10.5194/acp-8-6117-2008.

Zhang, R. Y., X. X. Tie, and D. W. Bond (2003), Impacts of anthropogenic and natural NOx sources over the US on tropospheric chemistry, *Proc. Natl. Acad. Sci. U. S. A.*, *100*(4), 1505–1509, doi:10.1073/pnas.252763799.

Zhang, R., G. Li, J. Fan, D. L. Wu, and M. J. Molina (2007), Intensification of Pacific storm track linked to Asian pollution, *Proc. Natl. Acad. Sci. U. S. A.*, *104*(13), 5295–5299, doi:10.1073/pnas.0700618104.

Ziemke, J. R., S. Chandra, and P. K. Bhartia (1998), Two new methods for deriving tropospheric column ozone from TOMS measurements: Assimilated UARS MLS/HALOE and convective-cloud differential techniques, *J. Geophys. Res.*, *103*(D17), 22,115–22,127, doi:10.1029/98JD01567.

Ziemke, J. R., S. Chandra, B. N. Duncan, L. Froidevaux, P. K. Bhartia, P. F. Levelt, and J. W. Waters (2006), Tropospheric ozone determined from aura OMI and MLS: Evaluation of measurements and comparison with the Global Modeling Initiative's Chemical Transport Model, *J. Geophys. Res.*, *111*, D19303, doi:10.1029/2006JD007089.

Zipser, E., D. Cecil, C. Liu, S. Nesbitt, and D. Yorty (2006), Where are the most intense thunderstorms on earth?, *Bull. Am. Meteorol. Soc.*, *87*(8), 1057–1071, doi:10.1175/BAMS-87-8-1057.